

**THE SENSITIVITY OF
R-PROCESS NUCLEOSYNTHESIS
TO THE PROPERTIES OF NEUTRON-RICH NUCLEI**

R. SURMAN*, M.R. MUMPOWER, J. CASS, and A. APRAHAMIAN

*Department of Physics, University of Notre Dame,
Notre Dame, IN 46556, U.S.A.*

**E-mail: rsurman@nd.edu
www.nd.edu*

About half of the heavy elements in the Solar System were created by rapid neutron capture, or r-process, nucleosynthesis. In the r-process, heavy elements are built up via a sequence of neutron captures and beta decays in which an intense neutron flux pushes material out towards the neutron drip line. The nuclear network simulations used to test potential astrophysical scenarios for the r-process therefore require nuclear physics data (masses, beta decay lifetimes, neutron capture rates, fission probabilities) for thousands of nuclei far from stability. Only a small fraction of this data has been experimentally measured. Here we discuss recent sensitivity studies that aim to determine the nuclei whose properties are most crucial for r-process calculations.

Keywords: nuclear reactions, nucleosynthesis, abundances

1. Introduction

Current and upcoming radioactive beam facilities will have the capability to measure basic nuclear properties, such as masses and beta decay rates, of many neutron-rich nuclei for the first time. These measurements have the potential to revolutionize our understanding of the evolution of nuclear structure far from stability. This understanding is crucial for many applications, including accurate models of the astrophysical processes in which these nuclei participate.

Rapid neutron capture, or r-process, nucleosynthesis is one such astrophysical process; see, e.g., Ref. 1 for a recent review. In the r-process, heavy nuclei are built up by a sequence of fast neutron captures and beta decays, where the timescale for captures is initially much faster than that for decays.² Thus nuclei quite far on the neutron-rich side of stability participate

in the process. We observe the resulting r-process abundance pattern in the solar system and in many old stars, e.g., Ref. 3. Exactly where astrophysically the r-process takes place, however, is still not conclusively determined.^{1,4}

Investigating potential astrophysical sites for the r-process involves simulations that require nuclear data for thousands of nuclei far from stability. Since as of yet only a small percentage has been measured experimentally, we rely on theoretical models for this data. There is a long tradition of examining the impact of various choices of global nuclear models on shaping the r-process abundance pattern; see Refs. 1,5 and references therein. Complementary to these efforts are r-process sensitivity studies, which aim to understand the role of *individual* pieces of nuclear data on r-process dynamics and to point out the nuclei whose properties play the most important role shaping the final abundance pattern. The latter can potentially guide upcoming radioactive beam experiments by indicating the pieces of nuclear data with the greatest astrophysical impact.

Sensitivity studies have been performed for neutron capture rates,⁶⁻⁹ neutron separation energies,¹⁰ and beta decay rates.¹¹ Here we present a variation of the neutron separation energy study and examine the dependence of this and the beta decay studies upon the potential r-process astrophysical conditions.

2. Sensitivity studies

We begin our sensitivity studies by choosing a baseline r-process simulation that produces a final abundance pattern that is a reasonable match to the solar pattern for $A > 120$. We then modify one piece of nuclear data—a single mass or beta-decay rate, for example—and repeat the simulation. The final mass fractions of this simulation $X(A)$ are compared to those of the baseline simulation $X_{\text{baseline}}(A)$ using a global sensitivity measure F :

$$F = 100 \times \sum_A |X_{\text{baseline}}(A) - X(A)|. \quad (1)$$

The mass fractions are related to the abundances $Y(A)$ by $X(A) = AY(A)$, and $\sum_A X(A) = 1$. This process is repeated for every mass or beta decay rate, resulting in a sensitivity measure F determined for each nucleus in the network.

For the r-process simulations we use the nuclear network code from Ref. 12. It is a dedicated r-process network code that includes neutron captures, photodissociations, beta decay, and beta-delayed neutron emission

(and neutrino interactions and fission, though these options are not used for the sensitivity studies described here). We use nuclear masses from Ref. 13 (FRDM), Ref. 14 (DZ), or Ref. 15 (HFB-21), and neutron capture rates consistent with these mass sets from Refs. 16, or calculated with TALYS.¹⁷ Beta decay rates are from Ref. 18.

3. Binding energy study

The study described here is based on the neutron separation energy sensitivity study of Ref. 10. Neutron separation energies appear explicitly in the calculation of photodissociation rates via detailed balance:

$$\lambda_\gamma(Z, A) \propto T^{3/2} \exp\left[-\frac{S_n(Z, A)}{kT}\right] \langle\sigma v\rangle_{(Z, A-1)} \quad (2)$$

where T is the temperature, $\langle\sigma v\rangle_{(Z, A-1)}$ is the thermally-averaged neutron capture cross section for the nucleus with one less neutron, and $S_n(Z, A)$ is the neutron separation energy—the difference in binding between the nuclei (Z, A) and $(Z, A - 1)$. In Ref. 10, the neutron separation energies, as they appear in the equation above, were varied from their theoretical values by $\pm 25\%$. The sensitivity study proceeded as described in Sec. 2 above, for astrophysical conditions chosen to be similar to those of Ref. 19.

One stated aim of the study in Ref. 10 was to highlight individual nuclear masses important for the r-process that are within reach of current and next generation experiments. The sensitivity study results presented in Fig. 3 of Ref. 10 do not give the full picture, however, since each separation energy depends on two different nuclear masses. Therefore here we repeat this study, varying individual *masses* rather than separation energies. Once the mass is varied, the two separation energies that depend on that mass are adjusted accordingly, and the r-process baseline simulation is repeated with this variation in the nuclear data. The results are presented in Fig. 1.

Figure 1 shows the same bulk features as Fig. 3 of Ref. 10. The largest sensitivity measures F are produced by variations in the masses of nuclei along and near the r-process path, particularly at the closed shells. While equilibrium persists between neutron captures and photodissociations, the masses determine abundances along each isotopic chain, and the relative abundances of the isotopic chains are set by beta decays. A change to a mass along the chain has the biggest impact on the overall r-process abundance pattern if it alters the location of the path and additionally the rate at which material moves out of the chain via beta decay. This is described in more detail in Ref. 10.

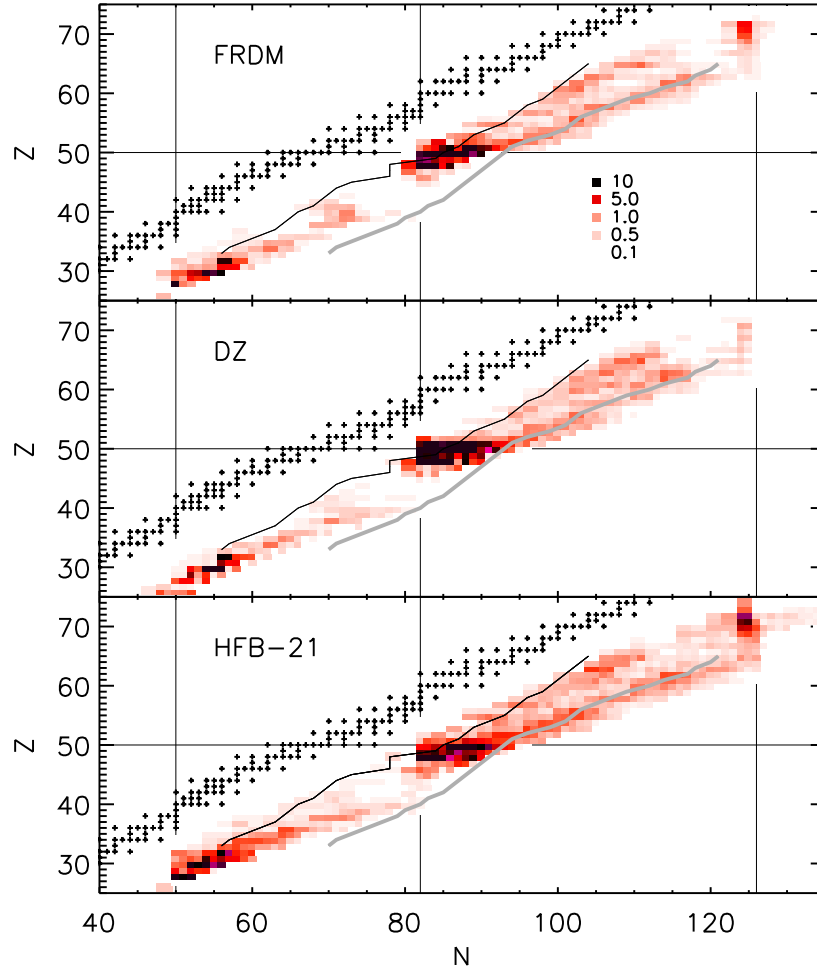


Fig. 1. Sensitivity measures F for each nucleus (Z, N) in the network, for three binding energy sensitivity studies using FRDM¹³ (top panel), DZ¹⁴ (middle panel), and HFB-21¹⁵ (bottom panel) masses. All three studies use binding energy variations of ± 1 MeV and astrophysical conditions as used in Ref. 10. Overlaid are estimated 10^{-4} fission yields for CARIBU²⁰ (thin black line) and FRIB²¹ (wide grey line).

The major difference between Fig. 1 and Fig. 3 of Ref. 10 concerns the results for nuclei closer to stability than the equilibrium r-process path. These nuclei are populated at later times in the r-process, as $(n, \gamma) - (\gamma, n)$ equilibrium fails, material moves toward stability, and neutron captures,

photodissociations, and beta decays all compete to shape the final abundance pattern. A variation in a neutron separation energy produces a variation in the photodissociation rate (Eq. (2)); this can alter the late time nuclear flow, particularly if the nucleus with the varied rate is populated and has fallen out of equilibrium. Ref. 7 describes this late-time photodissociation effect. Since odd- N nuclei tend to fall out of equilibrium much earlier than even- N nuclei, their photodissociation rates, and thus their neutron separation energies, tend to be more important at these late times. The sensitivity measures in Fig. 3 of Ref. 10 showed just this expected odd-even behavior. It is missing from Fig. 1, however, because in the binding energy sensitivity study a variation in an odd- N separation energy is produced when the binding energy of the odd- N nucleus or its adjacent even- N neighbor is altered. Thus while Fig. 3 of Ref. 10 highlights an interesting feature of r-process dynamics, the new Fig. 1 more accurately gauges the potential import of individual mass measurements on the r-process pattern.

4. Dependence on astrophysical conditions

Given the mechanisms by which individual pieces of data influence the r-process abundance pattern described in Refs. 6–11 and briefly above, it is expected that the sensitivity measures F will be strongly dependent upon the baseline r-process astrophysical conditions chosen for the study. For example, consider the case outlined in Sec. 3 above. The equilibrium mechanism operates most strongly along the r-process path, which is set by the temperature and neutron number density. Repeating the study with different temperature and density conditions should therefore shift the nuclei with the highest sensitivity measures F to correspond to the new path. The late-time photodissociation effect operates as equilibrium is failing but before the temperature has dropped so much that photodissociation is shut off entirely. The range of nuclei for which this effect produces noticeable changes to the final abundance pattern is thus sensitively tied to the late-time evolution of the temperature and density.²²

To examine these effects, we repeat the sensitivity study of Sec. 3 three times, varying the baseline astrophysical conditions each time. We choose the adiabatic wind parameterization of Ref. 23 as implemented in Ref. 22, where the density as a function of time is given by:

$$\rho(t) = \rho_1 \exp(-t/\tau) + \rho_2 \left(\frac{\Delta}{\Delta + t} \right)^2, \quad (3)$$

where $\rho_1 + \rho_2$ is the density at time $t = 0$, $3\tau = \tau_{\text{dyn}}$, and Δ is a constant real

6

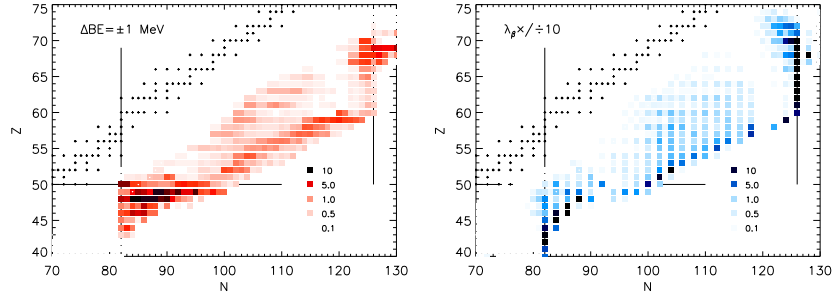


Fig. 2. Sensitivity measures F for each nucleus (Z, N) in the network, for the binding energy (left) and beta decay (right) sensitivity studies described in Sec. 4. The studies use FRDM masses and a wind parameterization from Ref. 9 with entropy $s/k = 10$ and initial electron fraction $Y_e = 0.150$.

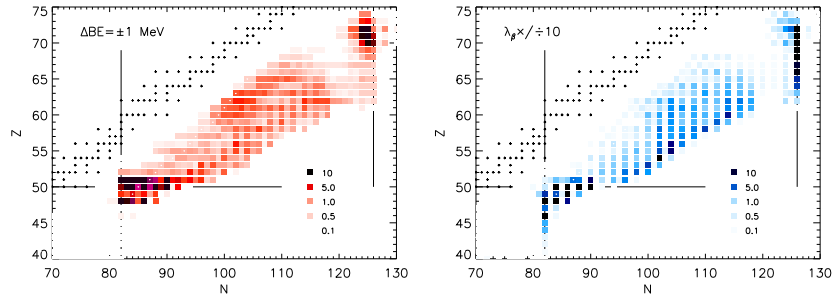


Fig. 3. Similar to Fig. 2, except with wind parameters $s/k = 100$ and $Y_e = 0.250$.

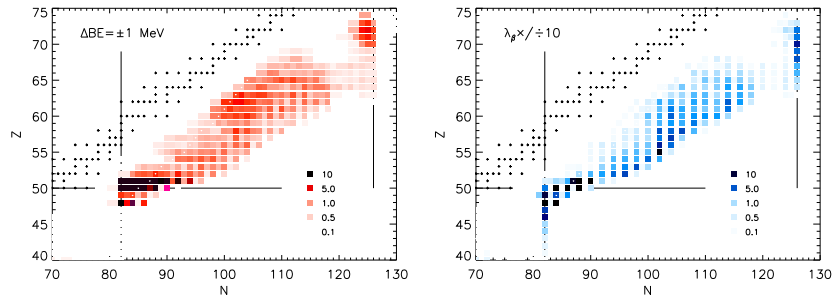


Fig. 4. Similar to Fig. 2, except with wind parameters $s/k = 200$ and $Y_e = 0.300$.

number. Our choices for these parameters here are $\rho(0) = 1.58 \times 10^8 \text{ g/cm}^3$, $\tau_{\text{dyn}} = 80 \text{ ms}$, and $\Delta = 10 \text{ ms}$. The temperature is determined from the density and the choice of entropy, and the initial composition is determined by the choice of electron fraction Y_e . Here we select three combinations of

entropy and initial electron fraction that produce a main r-process pattern similar to solar as our baseline simulations for the sensitivity studies. The results are shown in the left panels of Figs. 2-4.

At a given density, a lower entropy trajectory has a lower temperature than a higher entropy trajectory. In addition, lower entropy trajectories requires a greater neutron richness to make a successful main r-process. Both of these effects act in the same direction, such that the lowest entropy trajectory considered has a path farthest from stability, while the path for the highest entropy trajectory is closest to stability. As a result, the greatest F measures in the binding energy study show the same behavior—they are shifted far from stability for the low entropy trajectory (Fig. 2) and closer to stability in the high entropy trajectory (Fig. 4). In addition, higher temperatures persist longer in the higher entropy trajectory, so photodissociation rates continue to be important even quite close to stability.

In addition to repeating the binding energy study, for the same hydrodynamics we run three beta decay sensitivity studies as in Ref. 11. Here the studies proceed as described in Sec. 2, for variations in the beta decay rates by a factor of 10. The results are shown in the right panels of Figs. 2-4. Beta decay sensitivity measures F tend to follow the abundances quite closely,¹¹ with the highest F measures generally seen for nuclei along the equilibrium r-process path. Thus, the greatest sensitivity measures evolve with entropy as described above. However, unlike the photodissociation rates that essentially turn off at low temperature, beta decay rates continue to be important through even later times, for as long as they compete with neutron capture. Thus individual beta decay rates quite close to stability are influential in all three choices of r-process conditions.

5. Conclusion

Sensitivity studies are useful tools to highlight pieces of nuclear data that are important for astrophysical processes. Here we have presented a new binding energy sensitivity study for the r-process and examined the impact of variations in astrophysical conditions on the results of this and a beta-decay sensitivity study. We note that a large number of the same nuclei show up as important, particularly at the closed shells and in the rare earth region close to stability, despite the differences in astrophysical conditions. Many of these nuclei are within the reach of current radioactive beam experiments.

Acknowledgements

This work was supported by the National Science Foundation under grant number PHY1068192 and through the Joint Institute for Nuclear Astrophysics grant number PHY0822648, and the Department of Energy under contract DE-FG02-05ER41398 (RS).

References

1. M. Arnould, S. Goriely, K. Takahashi, *Phys. Rep.* **450**, 97 (2007).
2. J.J. Cowan, F.-K. Thielemann, J.W. Truran, *Phys. Rep.* **208**, 267 (1991).
3. C. Sneden, J.J. Cowan, R. Gallino, *Ann. Rev. Astron. Astrophys.* **46**, 241 (2008).
4. Y.-Z. Qian, G.J. Wasserburg, *Phys. Rep.* **442**, 237 (2007).
5. A. Arcones, G. Martinez-Pinedo, *Phys. Rev. C* **83**, 045809 (2011).
6. J. Beun, J. C. Blackmon, W. R. Hix, G. C. McLaughlin, M. S. Smith, R. Surman, *J. Phys. G* **36**, 025201 (2009).
7. R. Surman, J. Beun, G.C. McLaughlin, W.R. Hix, *Phys. Rev. C* **79**, 045809 (2009).
8. R. Surman, M. Mumpower, G.C. McLaughlin, R. Sinclair, W.R. Hix, K.L. Jones, *Proceedings of the 14th International Symposium on Capture Gamma-Ray Spectroscopy and Related Topics*, World Scientific (2011).
9. M. Mumpower, G.C. McLaughlin, R. Surman, *Phys. Rev. C*, **86**, 035803 (2012).
10. S. Brett, I. Bentley, N. Paul, R. Surman, A. Aprahamian, *Eur. Phys. J. A* **48**, 184 (2012).
11. J. Cass, G. Passucci, R. Surman, A. Aprahamian, *Proceedings of Science*, PoS(NIC XII)154 (2012).
12. R. Surman, J. Engel, *Phys. Rev. C*, **64**, 035801 (2001).
13. P. Moller, J.R. Nix, W.D. Myers, W.J. Swiatecki, *Atomic Data Nucl Data Tables* **59**, 185 (1995).
14. J. Duffo, A.P. Zuker, *Phys. Rev. C* **52**, R23 (1995).
15. S. Goriely, N. Chamel, J.M. Pearson, *Phys. Rev. C* **82**, 035804 (2010).
16. T. Rauscher, F.-K. Thielemann, *Atomic Data Nucl Data Tables* **74**, 1 (2000).
17. S. Goriely, S. Hilaire, A.J. Koning, *Astron. Astrophys.* **487**, 767 (2008).
18. P. Moller, B. Pfeiffer, K.-L. Kratz, *Phys. Rev. C* **67**, 055802 (2003).
19. Y.-Z. Qian, P. Vogel, G.J. Wasserburg, *Astrophys. J* **494**, 285 (1998).
20. G. Savard, R. Pardo, *Proposal for the ^{252}Cf source upgrade to the ATLAS facility*, Technical report, ANL (2005).
21. O.B. Tarasov, M. Hausmann, *LISE++ development: Abrasion-Fission*, Technical report MSUCL1300, NSCL (2005).
22. M.R. Mumpower, G.C. McLaughlin, R. Surman, *Phys. Rev. C* **85**, 045801 (2012).
23. B.S. Meyer, *Phys. Rev. Lett.* **89**, 231101 (2002).